Konya Mühendislik Bilimleri Dergisi, c. 12, s.3, 737-755, 2024
Konya Journal of Engineering Sciences, v. 12, n. 3, 737-755, 2024
ISSN: 2667-8055 (Elektronic)
DOI: 10.36306/konjes.1496688

THEORETICAL INVESTIGATION FOR YTTERBIUM EFFECT ON RADIATION SHIELDING CHARACTERISTICS OF $50Bi_2O_3$-$15Li_2O$-$15PbO$-$(20-X)B_2O_3$-Yb_2O_3 BORATE GLASSES

[1]Murat AYGÜN, [2,*]Zeynep AYGÜN, [3]İbrahim HAN, [4]Emine NARMANLI HAN

[1] *Bitlis Eren University, Arts&Sciences Faculty, Physics Department, Bitlis, TÜRKİYE*
[2*] *Bitlis Eren University, Vocational School of Technical Sciences, Bitlis, TÜRKİYE*
[3] *Ağrı Ibrahim Cecen University, Arts&Sciences Faculty, Physics Department, Ağrı, TÜRKİYE*
[4] *Ağrı Ibrahim Cecen University, Vocational School, Ağrı, TÜRKİYE*
[1]maygun@beu.edu.tr, [2]zaygun@beu.edu.tr , [3]ihan@agri.edu.tr, [4]enhan@agri.edu.tr

Highlights

- Radiation shielding characteristics of ytterbium doped glasses have been studied.
- Phy-X/PSD, PAGEX, ESTAR, and SRIM codes have been used.
- Increasing amount of ytterbium exhibited higher shielding performances.

Graphical Abstract

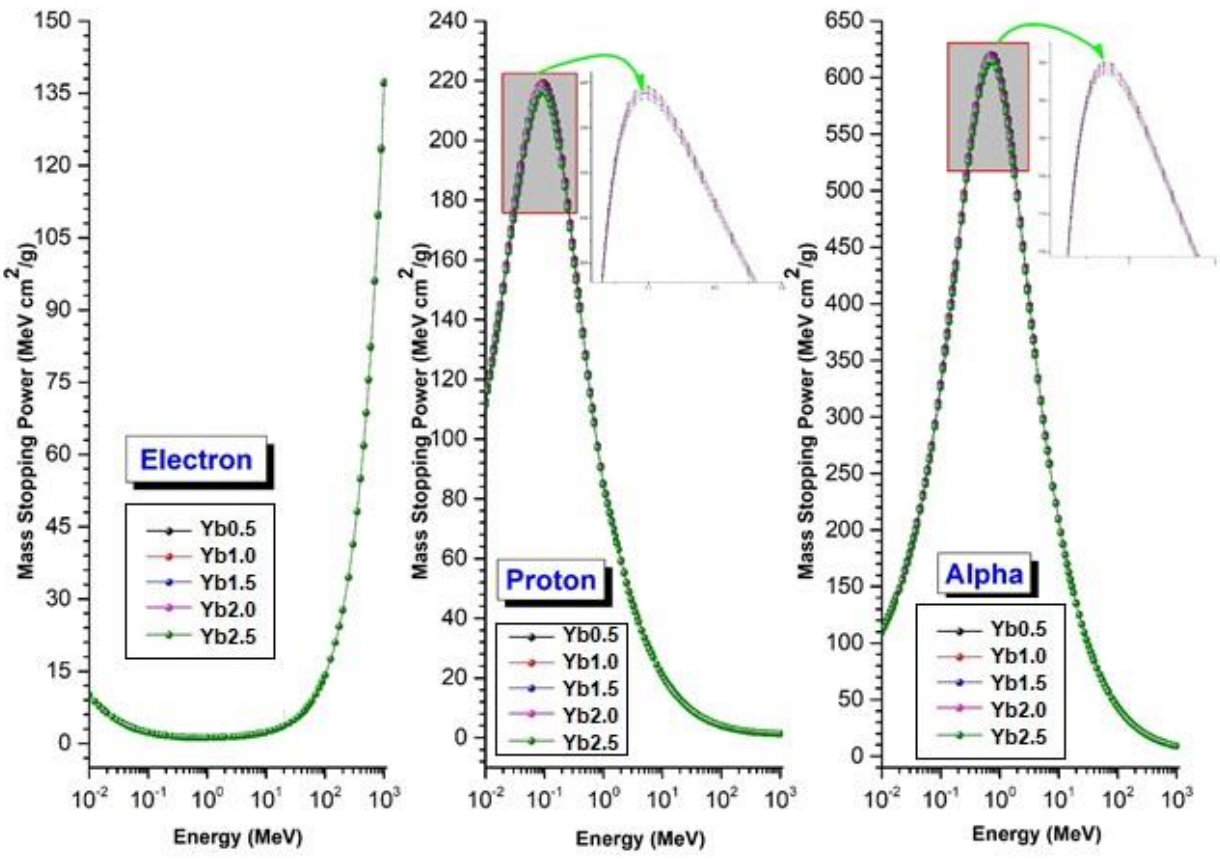

Dependence of MSP values of alpha, proton and electron particles versus the energy.

***Corresponding Author:** Zeynep AYGÜN, zaygun@beu.edu.tr

Konya Mühendislik Bilimleri Dergisi, c. 12, s.3, 737-755, 2024
Konya Journal of Engineering Sciences, v. 12, n. 3, 737-755, 2024
ISSN: 2667-8055 (Elektronic)
DOI: 10.36306/konjes.1496688

THEORETICAL INVESTIGATION FOR YTTERBIUM EFFECT ON RADIATION SHIELDING CHARACTERISTICS OF $50Bi_2O_3$-$15Li_2O$-$15PbO$-$(20-X)B_2O_3$-Yb_2O_3 BORATE GLASSES

[1]Murat AYGÜN, [2,*]Zeynep AYGÜN, [3]İbrahim HAN, [4]Emine NARMANLI HAN

[1] Bitlis Eren University, Arts&Sciences Faculty, Physics Department, Bitlis, TÜRKİYE
[2*] Bitlis Eren University, Vocational School of Technical Sciences, Bitlis, TÜRKİYE
[3] Ağrı Ibrahim Cecen University, Arts&Sciences Faculty, Physics Department, Ağrı, TÜRKİYE
[4] Ağrı Ibrahim Cecen University, Vocational School, Ağrı, TÜRKİYE
[1]maygun@beu.edu.tr, [2]zaygun@beu.edu.tr , [3]ihan@agri.edu.tr, [4]enhan@agri.edu.tr

(Received: 06.06.2024; Accepted in Revised Form: 07.08.2024)

ABSTRACT: As the nuclear industry has developed and radiation technologies have become more widely used, the dose of radiation from both synthetically produced sources and radioisotopes has increased, as has the number of people being irradiated. It is of the utmost importance to utilise appropriate shielding materials in order to reduce the negative effects of radiation sources. Doped glasses are among the most significant candidate materials in the field of radiation shielding. To this end, it was aimed to investigate the charged particle, gamma-ray and neutron shielding characteristics of ytterbium doped glasses with composition of $50Bi_2O_3$-$15Li_2O$-$15PbO$-$(20-x)B_2O_3$-Yb_2O_3 (where x = 0.5, 1.0, 1.5, 2.0 and 2.5). In this regard, the radiation shielding parameters were estimated by using Phy-X/PSD, PAGEX, ESTAR, and SRIM codes. Furthermore, the results were compared comprehensively and comparatively. Charged particle (alpha, proton and electron), gamma ray and neutron shielding efficiencies were found to be proportional to ytterbium content. The glasses with the increasing amount of ytterbium exhibited higher shielding performances. It can be said that all the studied glasses and particularly Yb2.5 sample could be used as shielding materials in many radiation related applications.

Keywords: *Borate Glass, Charged Particle Shielding, Gamma Shielding, Neutron Shielding, Yb*

1. INTRODUCTION

The group of rare earth elements (REs) is widely used in glass, ceramics, metallurgical industry, laser production, magnet production, oil catalyst and high-tech devices [1-6]. Ytterbium (Yb^{3+}), a rare earth (RE) element, has the potential to be utilized in the refinement of grains and the improvement of mechanical features of stainless steel products. With the half-life of 32 days, the radioactive isotope 169Yb is sometimes employed as a radiation source in the area of nuclear medicine. Alloys of ytterbium-iron-cobalt-manganese are appropriate for the production of high-quality permanent magnets. Similarly, ytterbium-doped crystals have the ability to act as dopant materials in lasers.

Glass is a material of great interest to researchers due to its many benefits, including its perfect corrosion resistance, hardness, optical properties and ease of processing by various techniques. Rare earth doped glass matrices can be a valuable alternative to glass materials for potential use as scintillators and non-leaded shields due to their low fabrication cost, chemical resistance, ease of fabrication and thermal stability properties [1-4]. Bismuth glass is in demand because of its extraordinary properties in amplifiers, lasers, optical data storage devices, etc. It is evident that the bismuth-borate matrix represents an ideal host matrix for REs, with applications spanning a range of disciplines including optical fibers, optical data storage devices, display technology, lasers, medical diagnostics and sensors [5-8]. Thus, Bi-doped glasses attract great attention from researchers [9-11]. Bi_2O_3 doped silica borotellurite glasses were studied by Geidam et al. [9] and it is suggested that the glasses are mechanically and thermally stable for applications in radiation shielding. Also, effect of Bi2O3 on gamma ray shielding and structural properties of borosilicate glasses recycled from high pressure sodium lamp glass was investigated and it was reported that good results were obtained [10]. Additionally, the Yb^{3+} ions present within the glasses serve as

***Corresponding Author:** Zeynep AYGÜN, zaygun@beu.edu.tr

sensitizers for the various RE^{3+} ions, imparting the energy to increase the efficiency of emission, thereby imparting a dielectric nature to the glasses [8].

The use of glass doped with REs has become a key component in the development of photonic applications in modern life. In recent decades, there has been extensive investigation into the synthesis of materials doped with REs for application within lighting technologies. This is because of the necessity of improving the performance of solid-state devices, LEDs, lasers etc. [12]. It is also important to examine the influence of the external ionizing radiation on the glassy structures' microstructure. Learning about the interaction between radiation and glasses gives us enlightening information for the reaction of the glassy matrices to the radiation. The radiation features of the RE-doped glass matrix are strongly influenced by the composition of the host material and these features were commonly studied by the researchers [12-16]. In particular, it has been demonstrated in numerous studies that the addition of Yb^{+3} ions into glasses significantly enhances their capacity for effective protection [17-19]. The role of Yb2O3 in the radiation shielding properties of B2O3-TiO2-BaO glasses wes studied by Negm et al. [18], and it was obtained that this type of glass with low concentrations of Yb2O3 shows good shielding properties. Tamam et al. [19] reported that the photon shielding ability and dosimetry potential of the glass system improved with Yb3+ weight content of the glasses and they are recommended for gamma radiation inhibition functions such as nuclear waste container, structural and source shields.

In countries with developing economies, nuclear energy has become a significant aspect of the energy production landscape. The operation of the nuclear reactor will result in the release of highly penetrating and dangerous radiation. Accordingly, it is essential that the reactor site is safeguarded by an appropriate layer of protection. With the growth of the nuclear industry and the increasing utilisation of radiation technologies, it is therefore evident that the attenuation of radiation levels to ensure safety has become a crucial requirement. For this purpose, the goal of the study is to analyze the radiation-glasses interaction characteristics and to obtain the radiation attenuation parameters (RAP), which are significant to have the knowledge of attenuating abilities of the glasses, including the mass and linear attenuation coefficient values (MACVs and LACVs), mean free path value (MFPV), half value layer value (HVLV), electronic and atomic cross sections (ECS and ACS), effective and equivalent atomic number (Z_{eff} and Z_{eq}), effective electron density and conductivity (N_{eff} and C_{eff}), buildup factors (BUF), KERMA, fast neutron removal cross section value (FNRCSV), the mass stopping power (MSP) and projected range (Rp). In this context, the RAP of $50Bi_2O_3$-$15Li_2O$-15PbO-(20-x)B_2O_3-Yb_2O_3 (x = 0.5, 1.0, 1.5, 2.0 and 2.5 mol%) glasses are evaluated by Phy-X/PSD [20], SRIM [21], PAGEX [22] and ESTAR (Institute) codes in different energies.

2. MATERIAL AND METHODS

The knowledge necessary for the computations of glass samples were taken from Ref. Bhemarajam et al. [8] to ascertain their potential for radiation shielding. The glasses with a composition of $50Bi_2O_3$-$15Li_2O$-15PbO-(20-x)B_2O_3-Yb_2O_3 (x = 0.5, 1.0, 1.5, 2.0 and 2.5 mol%) have been obtained using the melt quenching technique. In melt quenching technique, firstly, the chemicals were weighted according to mol percent, then, they were ground to homogeneity using an agate mortar and placed into an alumina crucible. The obtained mixture is melted in an electric furnace at high temperatures. The desired melts were then quenched using a preheated brass plate and a quencher to produce a glass sample. Glass samples were annealed to avoid unwanted thermal stress and air bubbles in the synthesised glass [8]. Table 1 presents the densities, chemical compositions and molar volumes of the chosen glasses. The samples are labeled as Yb0.5, Yb1.0, Yb1.5, Yb2.0 and Yb2.5 for x = 0.5, 1.0, 1.5, 2.0 and 2.5 mol%, respectively. The study [8] outlines the methodology employed to prepare and assess the physical characteristics of the studied samples.

Table 1. The elemental components and density of the glasses [8].

Sample	Bi	O	B	Li	Pb	Yb	Density (g/cm³)
Yb0.5	0.7295	0.1340	0.0147	0.0073	0.1085	0.0060	5.302
Yb1.0	0.7253	0.1333	0.0143	0.0072	0.1079	0.0120	5.403
Yb1.5	0.7213	0.1325	0.0138	0.0072	0.1073	0.0179	5.523
Yb2.0	0.7173	0.1318	0.0134	0.0071	0.1067	0.0238	5.635
Yb2.5	0.7133	0.1311	0.0129	0.0071	0.1061	0.0295	5.794

2.1. Radiation protection parameters for the interaction of charged and uncharged particles with matter

The Beer–Lambert statement can be written to determine MACVs,

$$I = I_0 e^{-\mu t} \quad (1)$$

$$\mu_m = \frac{\mu}{\rho} = ln(I_0/I)/\rho t = ln(I_0/I)/t_m \quad (2)$$

LACVs and MACVs are accepted as μ (cm−1) and μm (cm2/g), respectively. The MACV is the potential for interaction between photons and the mass per unit area of a material, which provides insight into the absorption characteristics of the material in question. LACV is the fraction of incident photons attenuated per unit material thickness.

The HVLV refers to the capacity of radiation to penetrate a given substance. MFPV quantifies the average lenght traversed by radiation between two consecutive collisions within a given medium. HVLV and MFPV are calculated with the following equations

$$\mathrm{HVLV} = \frac{In(2)}{\mu}, \qquad \mathrm{MFPV} = \frac{1}{\mu} \quad (3)$$

The interaction posibilities of electrons and atoms in a given volume of any given material is denoted by the symbols ECS and ACS, respectively. ACS (σa) and ECS (σe) can be acquired with the help of equations [23]

$$\mathrm{ACS} = \sigma_a = \frac{N}{N_A}(\mu/\rho), \qquad \mathrm{ECS} = \sigma_e = \frac{\sigma_a}{Z_{eff}} \quad (4)$$

A compound's atomic number is constituted by several elements; a compound with more than one element is referred to as an effective atomic number (Zeff). Zeff is obtained by [24]

$$\mathrm{Z_{eff}} = \sigma_a/\sigma_e \quad (5)$$

The Neff parameter is associated with the effective conductivity of the relevant material, which is dependent upon the excitatory photon energy. Ceff is in proportion to Neff. Neff and Ceff values can be written as

$$\mathrm{N_{eff}} = \frac{\mu_m}{\sigma_e}, \qquad \mathrm{C_{eff}} = \left(\frac{\mathrm{N_{eff}}\,\rho e^2 \tau}{m_e}\right) \times 10^3 \quad (6)$$

The Neff value of the charged particles (CPs) can be determined by replacing MAC with the MSP value [21].

BUF, energy absorption build up factor (EABF) and exposure build up factor (EBF), can be found by the following equations below [25-27].

$$Z_{eq} = \frac{Z_1(logR_2 - logR) + Z_2(logR - logR_1)}{logR_2 - logR_1} \quad (7)$$

$$F = \frac{F_1(logZ_2 - logZ_{eq}) + F_2(logZ_{eq} - logZ_1)}{logZ_2 - logZ_1} \quad (8)$$

$$B(E,x)\begin{cases} 1 + \frac{(b-1)(K^x-1)}{(K-1)} & \text{for } K \neq 1 \\ 1 + (b-1)x & \text{for } K = 1 \end{cases} \quad (9)$$

$$K(E,x) = cx^a + d\frac{\tanh\left(\frac{x}{X_k} - 2\right) - \tanh(-2)}{1 - \tanh(-2)} \quad \text{for } x \leq 40 \text{ mfp} \quad (10)$$

The R1 and R2 values represent the ratio of Compton scattering to total attenuation for adjacent elements with atomic numbers Z1 and Z2, measured in micrometres. F is a set of G-P FP (a, b, c, d, and XK coefficients) for the sample. F1 and F2 are the G-P FP for atomic numbers Z1 and Z2 at a specific energy. x and E refer to the penetration depth and primary photon energy, respectively.

In the case of glass systems, the KERMA with reference to air can be expressed as follows: [28]

$$\text{KERMA} = \frac{(\mu_{en}/\rho)_{glass}}{(\mu_{en}/\rho)_{air}} \quad (11)$$

The FNRCSV ($\sum R$) quantifies a material's potential capacity to attenuate neutrons and can be found by [20]

$$\sum R = \sum_i \rho_i (\sum R/\rho)_i \quad (12)$$

where ρ_i and $(\sum R/\rho)_i$ are the partial density of the glass and the mass removal cross-section of the ith constituent element, respectively.

SP can be formulated as [29]

$$\frac{dE}{dx} = 4\pi r_0^2 z^2 \frac{mc^2}{\beta^2} NZ \left[\ln\left(\frac{2mc^2}{I} \beta^2\gamma^2 \right) - \beta^2 \right] \quad (13)$$

and for electrons the SP formula is

$$\frac{dE}{dx} = 4\pi r_0^2 \frac{mc^2}{\beta^2} NZ \left\{ \ln\left(\frac{\beta\gamma\sqrt{\gamma-1}}{I} mc^2 \right) + \frac{1}{2\gamma^2}\left[\frac{(\gamma-1)^2}{8} + 1 - \left(\gamma^2 + 2\gamma - 1\right)\ln 2 \right] \right\} \quad (14)$$

The Rp value is assumed as

$$\text{Rp}(E) = \int_0^E \frac{1}{\left(-\frac{dE}{dx}\right)} dE \quad (15)$$

3. RESULTS and DISCUSSION

3.1. Radiation shielding analysis of charged and uncharged particles

The MACVs varied with photon energies were illustrated in Fig. 1(a). The MACRs exhibited a sharp reduction due to the photoelectric (PE) process at low energies (1-100 keV). At mid-energies (100 keV-5 MeV), they exhibited a slight change due to Compton scattering (CS). With increasing energy, the MACRs exhibited an increase due to pair production (PP) at high energies (>5 MeV) [30]. It can be said that the glasses protect well and Yb2.5 is slightly better than other results. The glasses shield equally well. Additionally, the LACVs that vary with photon energies were presented in Fig. 1(b), and the same shielding feature was found for the glasses. In Fig. 2, it is demonstated that the MACVs of the glasses have better shielding features especially at low energies than the previously investigated shield materials [31].

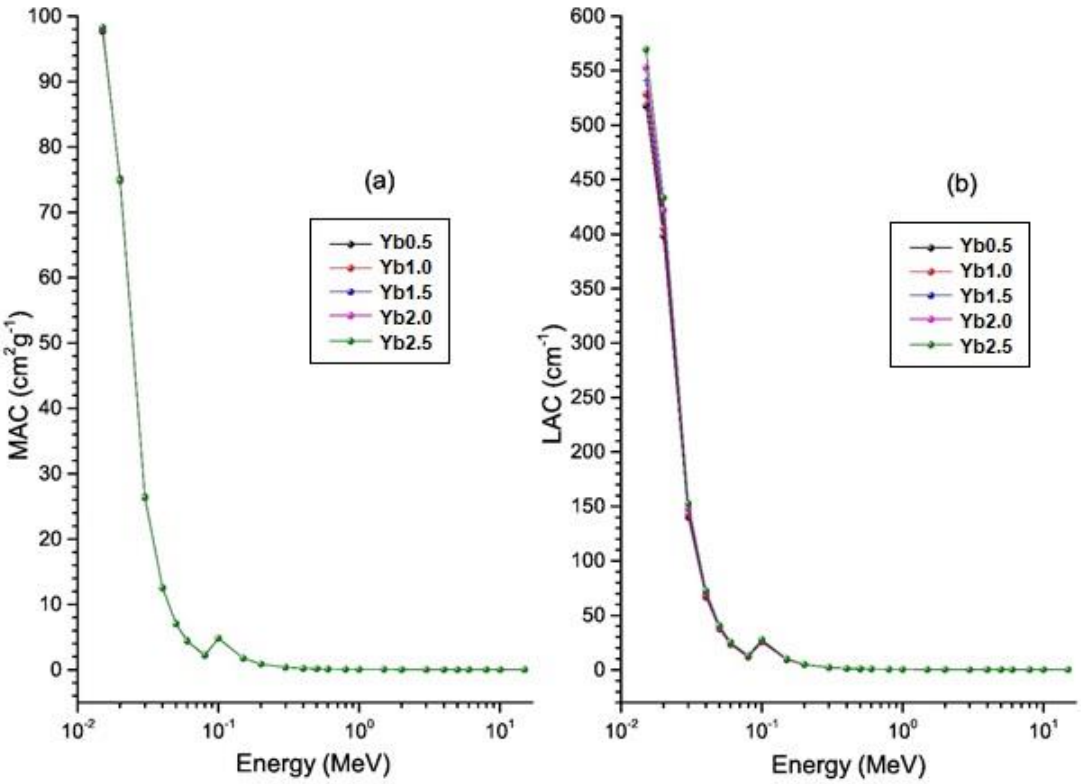

Figure 1. Variations of MAC (a) and LAC (b) values with photon energies.

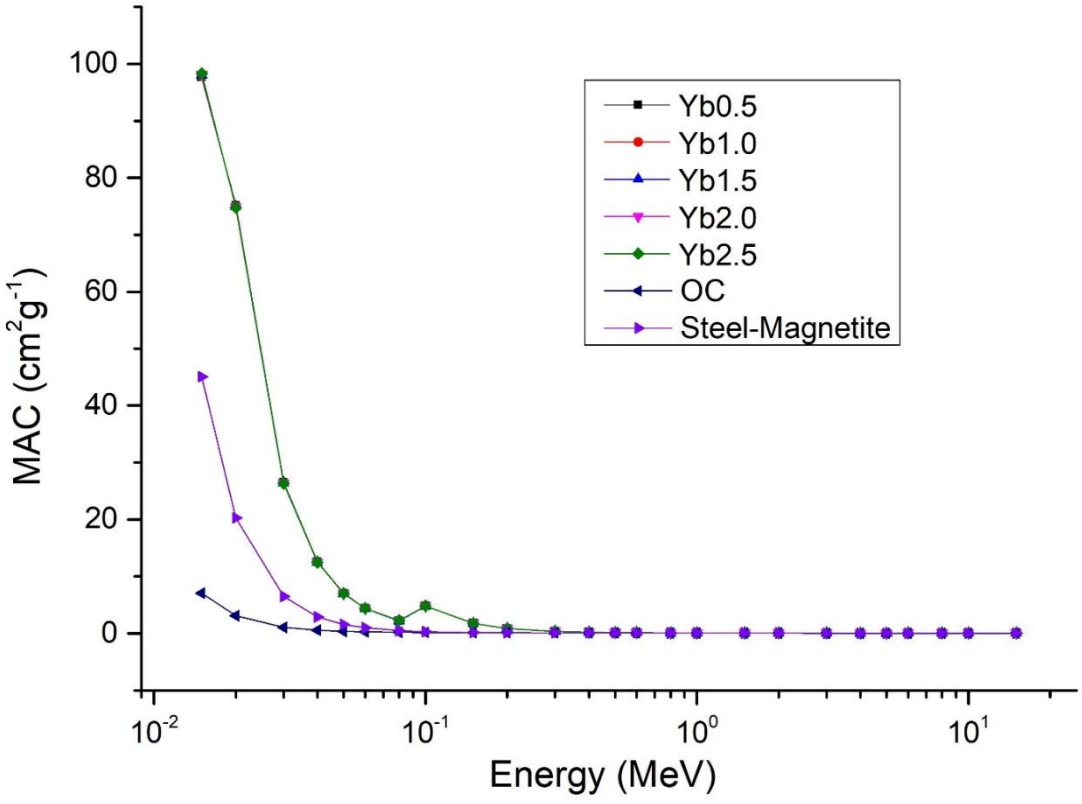

Figure 2. Comparison of MAC values of the glasses with previously studied shields.

The MFP and HVL results were exhibited in Figs. 3(a)-(b). At energies dominated by CS, photons were observed to exhibit a high probability of scattering. Consequently, thicker materials were found to be necessary, as they exhibited a lower probability of absorption and a greater photon MFPV. In the high energy region, lower HVL and MFP results were observed to be beneficial for enhanced shielding capability. In the high-energy region, lower HVL and MFP values are required, while in the lower energy region, thicker materials are necessary. In this regard, the MFP and HVL results are ordered as follows: Yb2.5 < Yb2.0 < Yb1.5 < Yb1.0 < Yb0.5. It is worth noting that glass Yb0.5 has the lowest level of shielding ability due to its high HVLVs and MFPVs, and Yb2.5 may offer the highest level of shielding among the glasses due to the lowest values. As seen in Fig. 4, the HVLVs of the studied glasses are lower than those of the materials reported before [31], so it can be said that the glasses are better protection materials.

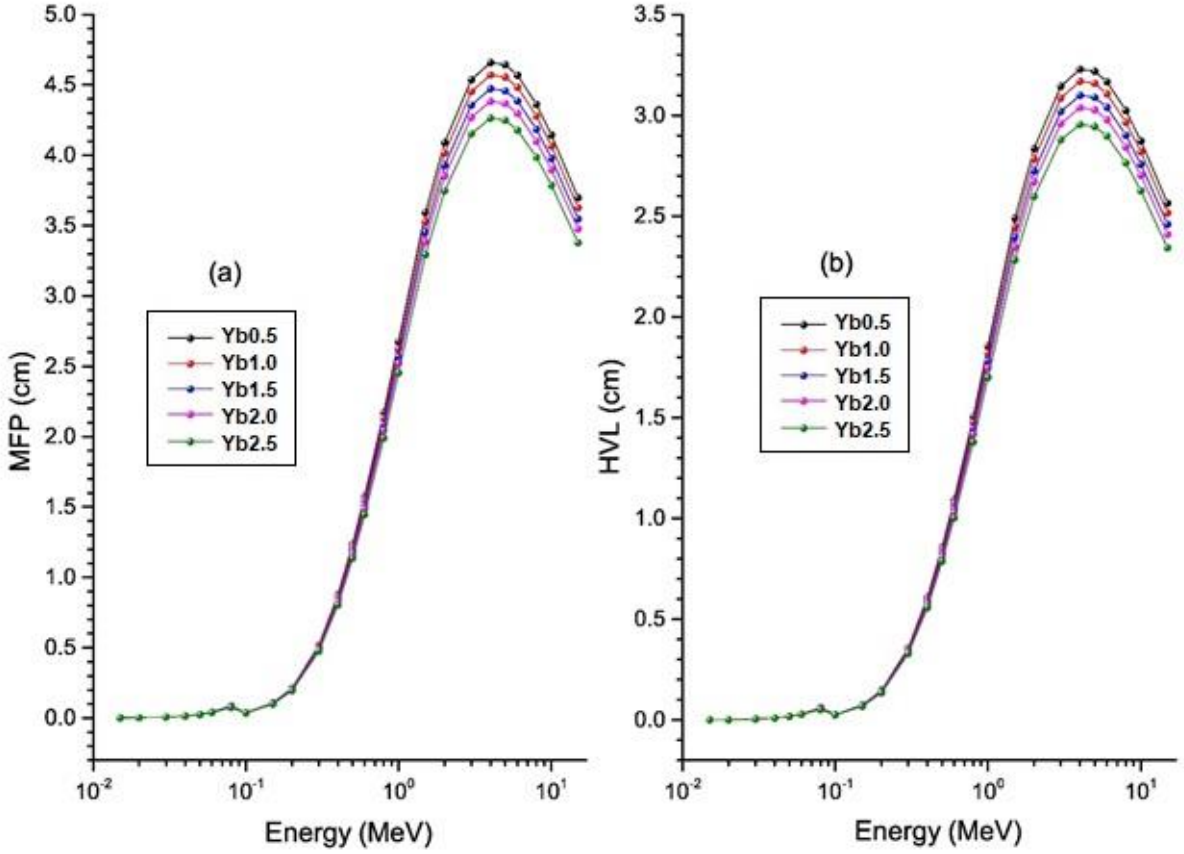

Figure 3. Variations of MFP (a) and HVL (b) values with photon energies.

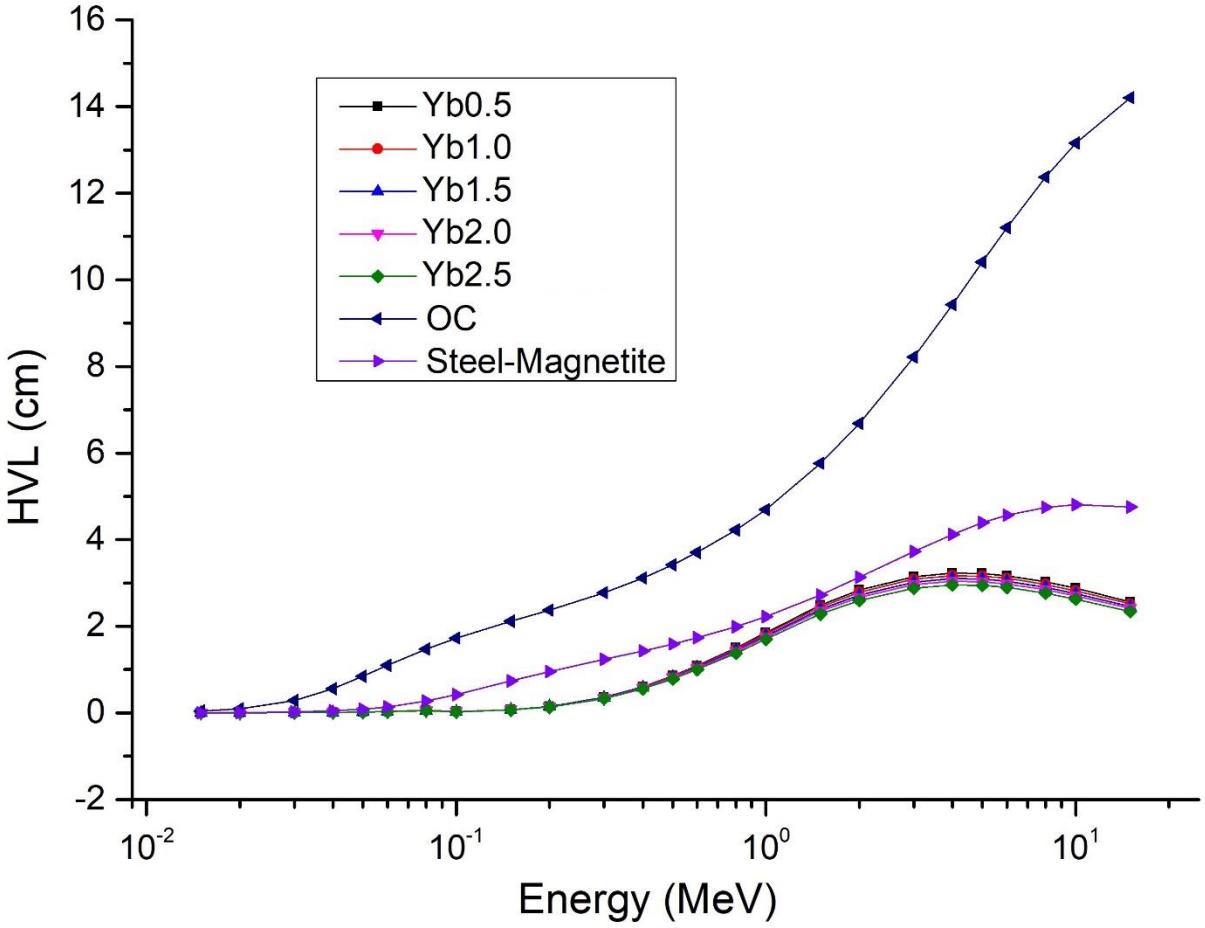

Figure 4. Comparison of HVLVs of the glasses with previously studied shields.

It can be of interest to enquire further into the interaction probabilities of a material, which are shown by ACS and ECS in Figs. 5(a) and (b). The results demonstrate that the ACS and ECS values exhibited a correlation with the energy of the photon. It can be postulated that the higher ACS and ECS results point to a better protective glass. It would appear that Yb2.5 has the highest protection character among all the glasses, based on the ACS and ECS values.

The Z_{eff} results, which is displayed in Fig. 6(a), gave the highest values because of the PE at low energy levels. The results exhibited a sharp decline and subsequent increase as the energy increases, before stabilizing at high energies. Glass with Yb2.5 composition, which contains a higher amount of Yb, shows the highest Z_{eff} values and thus the highest shielding performance. On the other hand, Yb0.5 with a lower Yb content show the lowest Z_{eff} values and the lowest protection ability. The Z_{eq} values of the glasses are displayed in Fig. 6(b). Yb2.5 presents a greater interaction, while Yb0.5 shows the least interaction between radiation and matter. The obtained values indicate that Yb2.5 exhibits a more pronounced interaction with radiation than Yb0.5, which demonstrates the least interaction among the glasses investigated. The Z_{eff} values of the glasses are also compared with those of the previous results reported for widely used shielding materials by Bashter [31]. The values are higher than the ordinary concrete (OC) and steel-magnetite, thus the proptection abilities are higher.

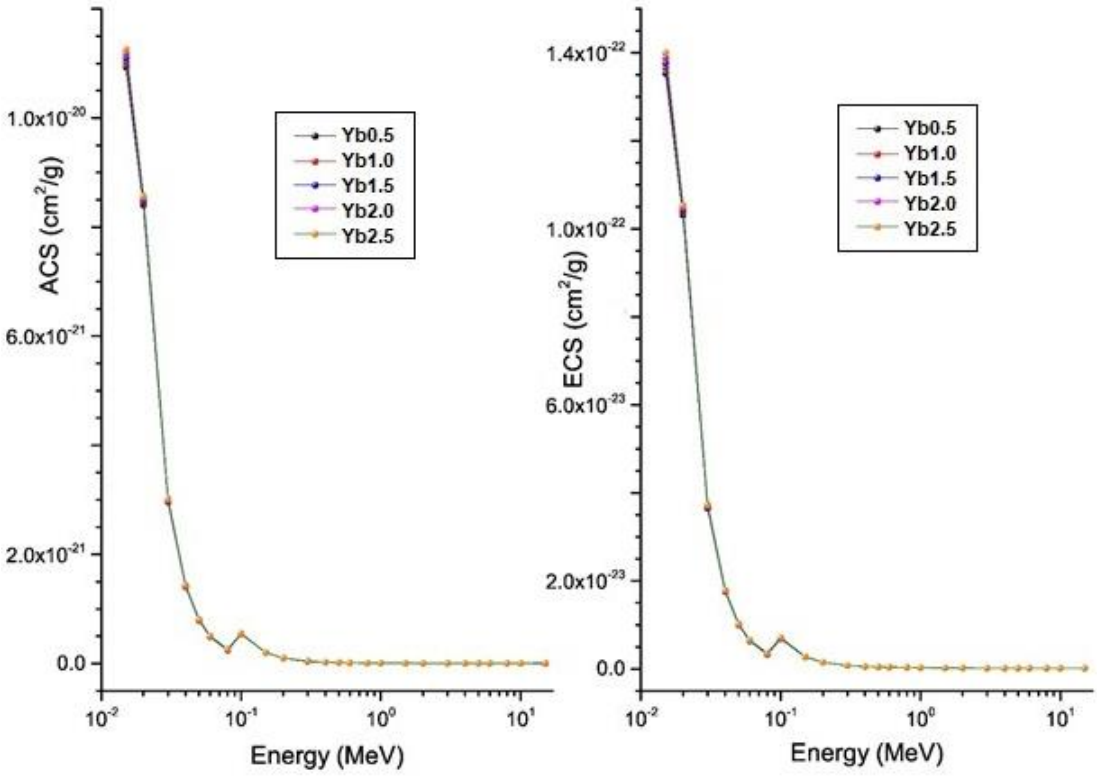

Figure 5. Variations of ACS (a) and ECS (b) values with photon energies.

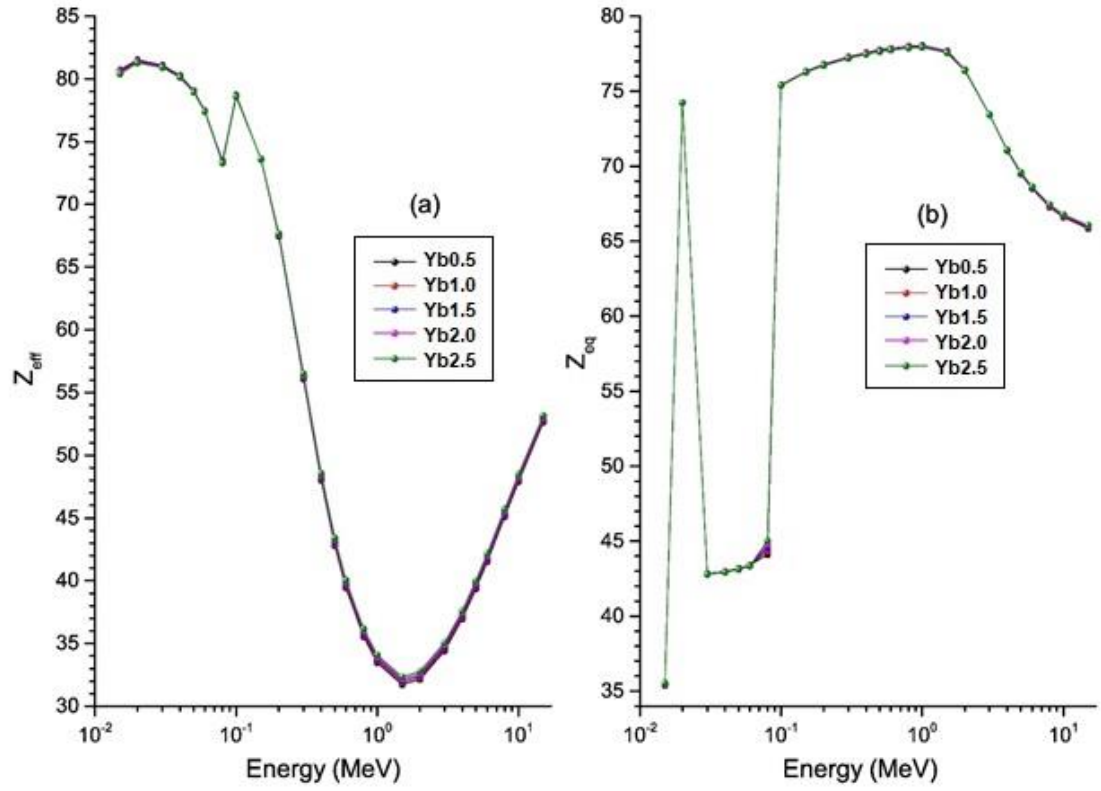

Figure 6. Changes of Z_{eff} (a) and Z_{eq} (b) values with photon energies.

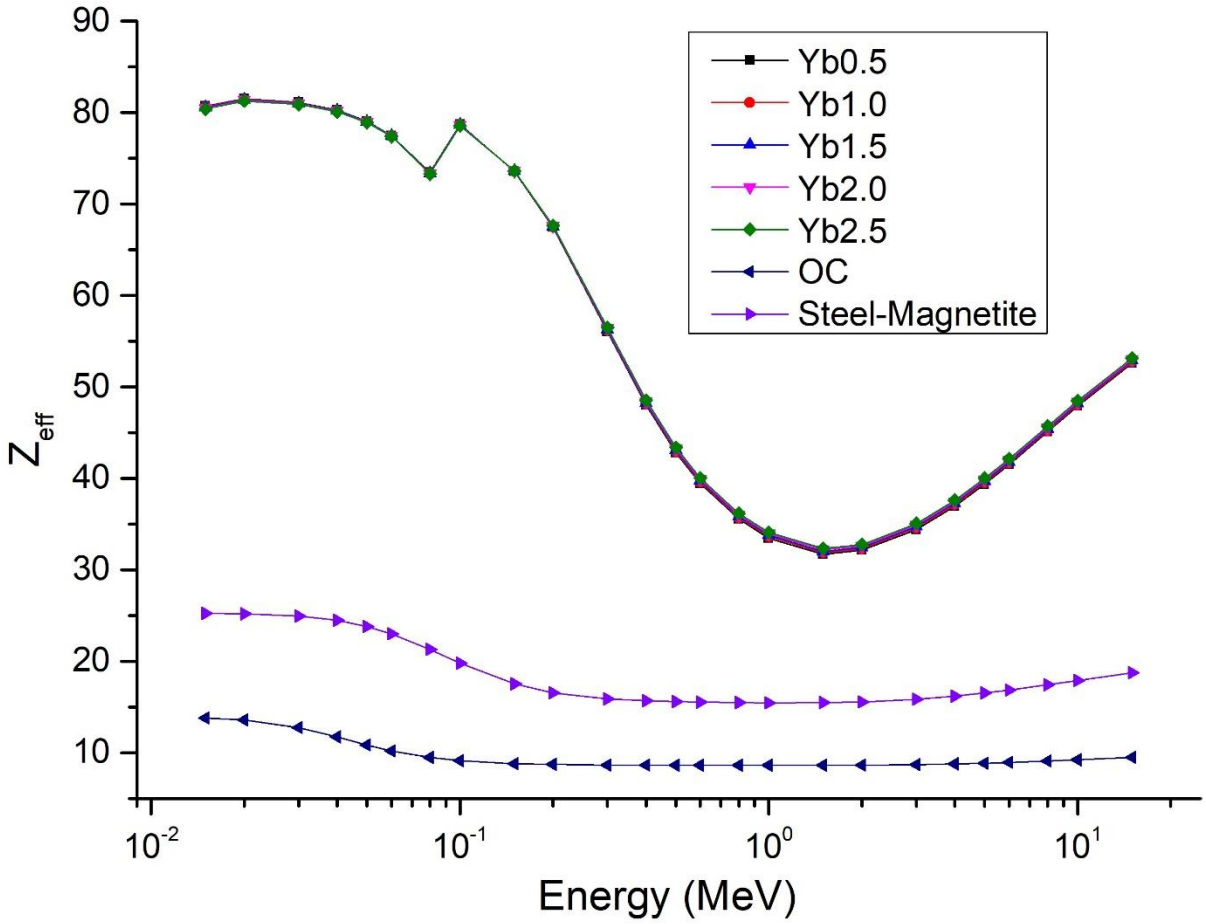

Figure 7. Comparison of Z_{eff} values of the glasses with previously studied shields.

Photon-material interactions result in alterations to the number of free electrons within the material, influenced by PE, CS, and PP interactions. This change is contingent upon the N_{eff} results, which correspond to the number of conduction electrons within the material. Consequently, C_{eff} is proportional to the N_{eff} of the glasses. The alterations in C_{eff} and N_{eff} results according to photon energies are illustrated in Figs. 8(a)-(b). It is noticed that Yb2.5 exhibits the highest C_{eff} and N_{eff} results among the glasses. The very sharp peak seen for Z_{eff}, C_{eff} and N_{eff} around 0.1 MeV can be attributed to the K absorption edges of the Bi and Pb elements [32].

The EABF and EBF of the glasses for 16 penetration depths were defined by the help of Phy-X/PSD and their changes with the incident energy are shown in Figs. 9 and 10, respectively. In the PE region, all energies absorb lower energy photons, resulting in small buildup factors. A large number of scattered photons in the CS region can cause the photon accumulation to increase, causing the factors to reach the highest values in the mid-energy region. The photon absorption rate is high in the PP region, which results in lower buildup factors in higher energy regions. The results indicate that the photon cluster for Yb0.5 is higher than that of the other glasses, as evidenced by the values obtained for EBF and EABF. Additionally, sharp increases in the energies at ≈0.03 and 0.1 MeV can be explained as L1 and K absorption edges of Bi [32].

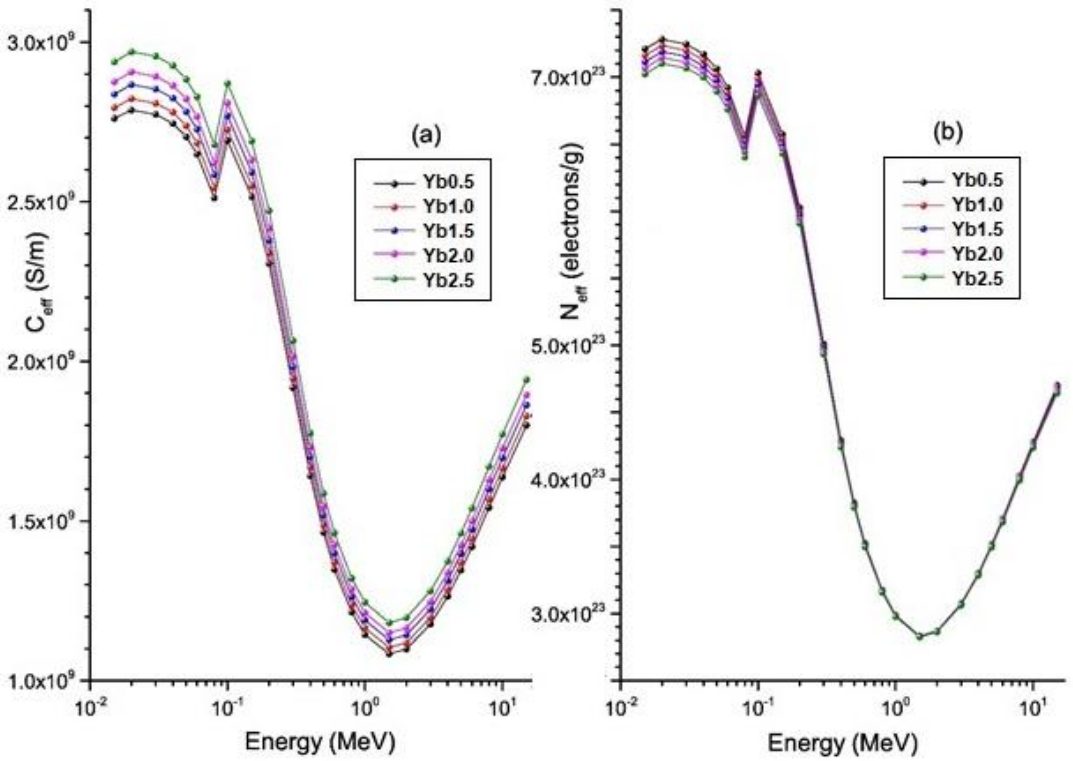

Figure 8. Changes of Ceff (a) and Neff (b) values with photon energies.

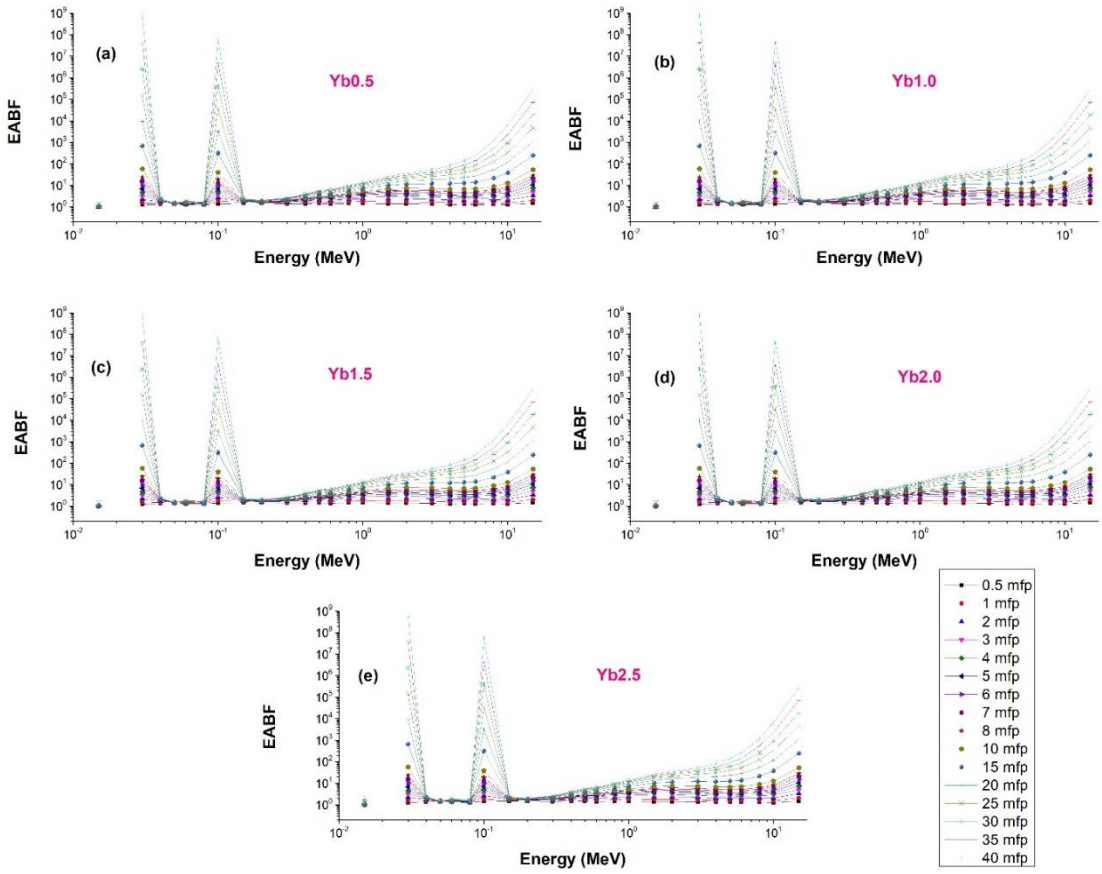

Figure 9. Variations of EABF values with photon energies.

The μen values are estimated and demonstrated in Fig. 11(a). The results (in cm^2/g) are in the range 0.022946 - 2266.293, 0.022941 - 2261.435, 0.022936 - 2256.637, 0.022932 - 2251.895 and 0.022927 - 2247.195 for Yb0.5, Yb1.0, Yb1.5, Yb2.0 and Yb2.5, respectively. The findings follow this order: Yb2.5 < Yb2.0 < Yb1.5 < Yb1.0 < Yb0.5. Additionally, the KERMA values are determined and shown in Fig. 11(b). At low energies, KERMA values are at their minimum, and begins to increase and reaches its highest value at 0.04 MeV. The data then demonstrated a rapid decline, followed by an average behavior. Yb0.5 achieved the greatest KERMA at 0.04 MeV while Yb2.5 had the lowest KERMA.

The neutron attenuation of the glasses is determined by means of the thermal and FNRCS values and shown in Fig. 12. Yb2.5 has the highest value and Yb0.5 the lowest for fast neutrons. The FNRCS values are compared with some shielding materials such as Bi20 glass, graphite and borogypsum reported previously and illustraded in Fig. 12 [30,33,34]. Unlike fast neutrons, thermal ones have the lowest value for Yb2.5 and the highest for Yb0.5. This phenomenon can be explained by the high content of heavy elements, for example bismuth, which do not have the capacity to absorb fast neutrons effectively within the glass composition. Given that B is an effective thermal neutron absorber [35], the elevated B_2O_3 concentration in the glass Yb0.5 has resulted in a notable enhancement in the glass's thermal neutron absorption capacity. It can be also seen that thermal neutron attenuation is better for Yb^{+3} doped glasses than that of cement mortar with 10% and 20%, replacement of borosilicate glass powder studied by Jang et al. [36].

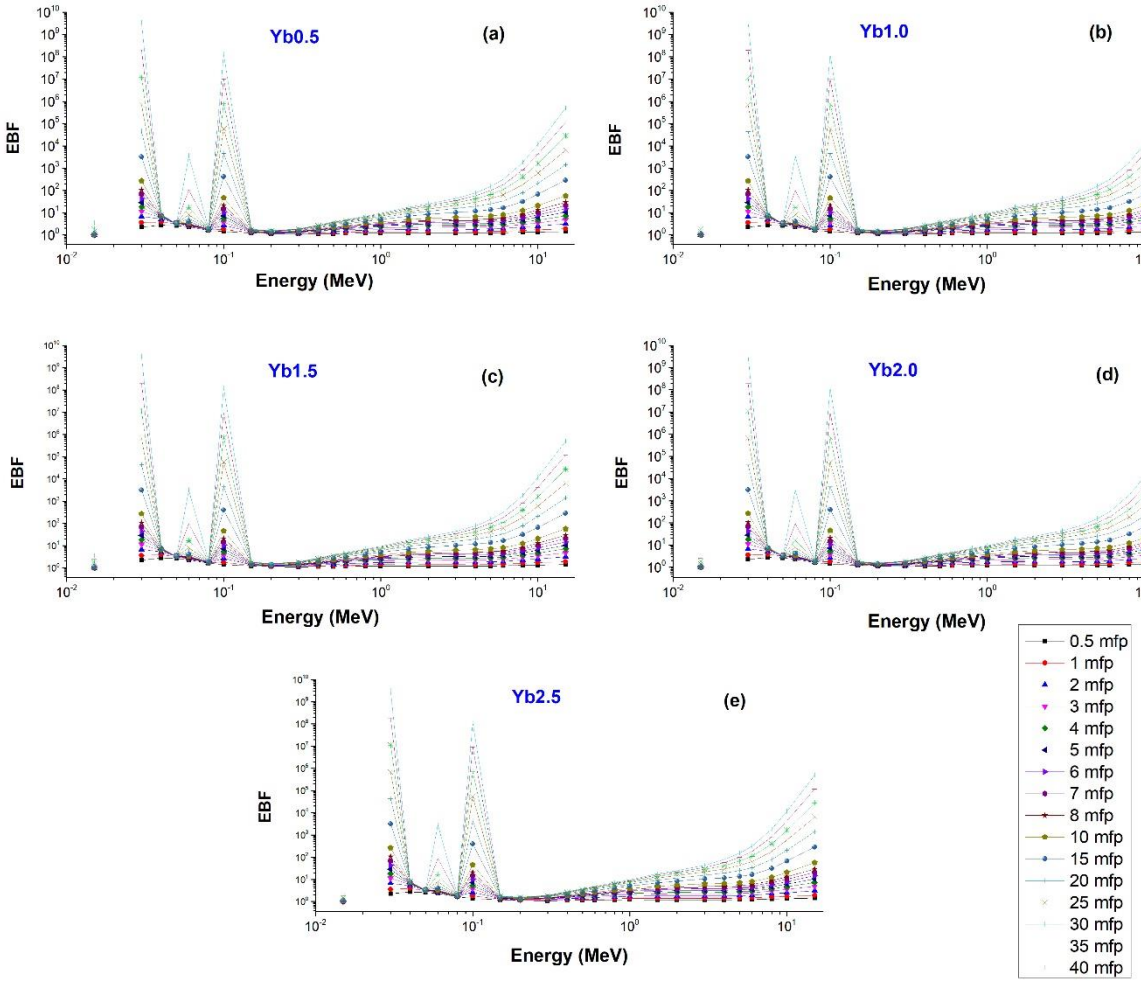

Figure 10. Variations of EBF values with photon energies.

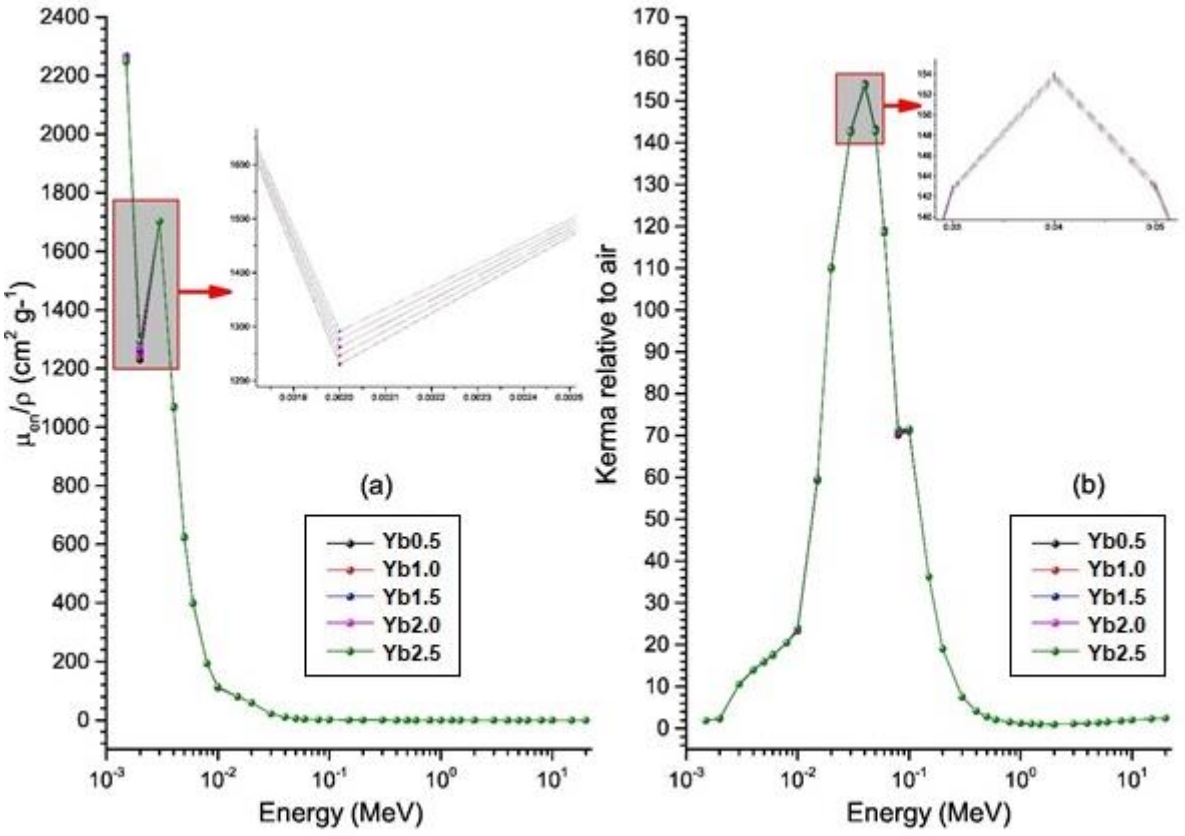

Figure 11. Variations of μen/ϱ (a) and KERMA relative to air (b) values with photon energies.

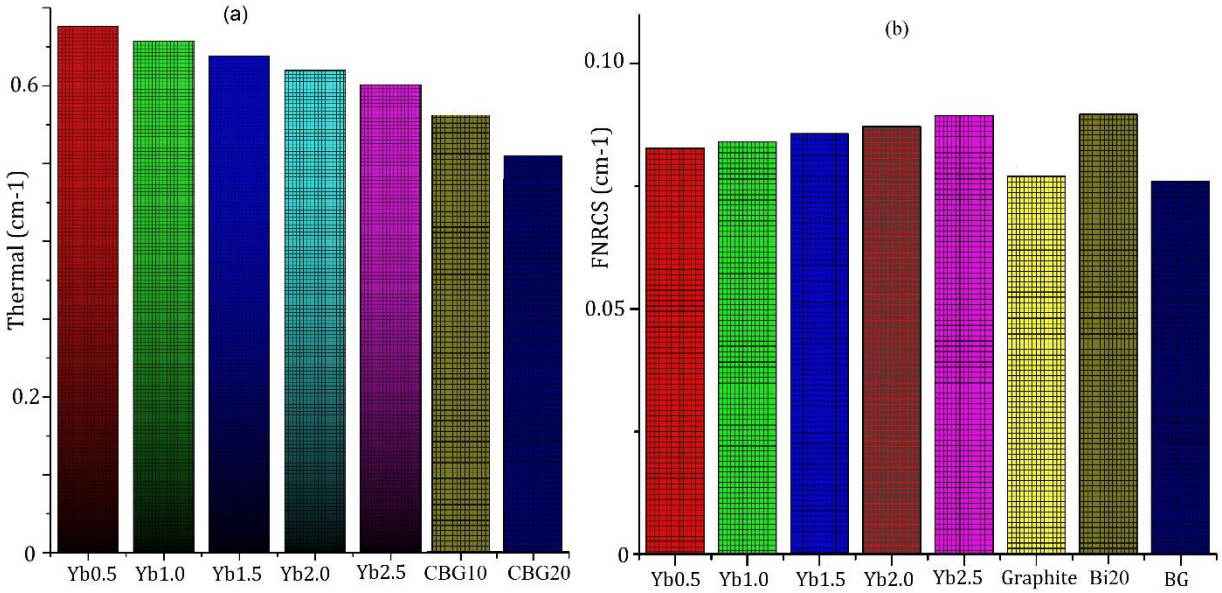

Figure 12. Comparison of thermal and FNRCS values of the glasses as comparative with previously reported materials.

The interaction of CPs with glasses is of paramount importance in radiation therapy. In order to ascertain the suitability of glasses for this aim, the MSP values of the electron, alpha and proton have been estimated for the glasses in question and the results have been presented in Fig. 13. The MSP values of electrons exhibit a decrease with increasing energy, followed by a gradual increase. In this case, the energy

loss mechanism of electrons is taken into account. It is supposed that electrons experience Coulomb interactions and bremsstrahlung. The MSP values (in MeV cm2/g) of electrons are among 1.196 – 137.0, 1.195 – 137.1, 1.194 – 137.2, 1.193 – 137.3 and 1.192 – 137.3 for Yb0.5, Yb1.0, Yb1.5, Yb2.0 and Yb2.5, respectively. MSP values for protons, increase with energy and subsequently, the value reduces in a gradual manner until the maximum is reached. The MSP results (in MeV cm2/g) of proton are among 1.306 – 219.136, 1.306 – 218.436, 1.305 – 217.735, 1.304 – 217.034 and 1.304 – 216.334 for Yb0.5, Yb1.0, Yb1.5, Yb2.0 and Yb2.5, respectively. The MSP for alpha particle exhibits an increase in energy prior to a subsequent decrease. It should be noted that the behavior of proton and alpha particles can be affected by the dependence of their electronic and nuclear energy losses, that in turn, can be influenced by the kinetic energy of the particles in question. The MSP values (in MeV cm2/g) of alpha are among 8.881 – 620.172, 8.877 – 618.671, 8.872 – 617.169, 8.868 – 615.668 and 8.863 – 614.166 for Yb0.5, Yb1.0, Yb1.5, Yb2.0 and Yb2.5, respectively. The MSP values for the glasses are given in the following order for the CPs: MSPelectrons < MSPprotons < MSPalpha.

The Rp results are calculated by performing the SRIM and the ESTAR codes at 0.01 - 30 MeV, and are displayed in Fig. 14. The Rp values (in μm) for electron are among 1.1976 – 22180, 1.1765 – 21765, 1.1522 – 21310, 1.1306 – 20887 and 1.1007 – 20331 for Yb0.5, Yb1.0, Yb1.5, Yb2.0 and Yb2.5, respectively. The Rp results (in μm) for proton are among 0.1082 – 3380, 0.1063 – 3320, 0.1042 – 3250, 0.1022 – 3180 and 0.0995 – 3100 for Yb0.5, Yb1.0, Yb1.5, Yb2.0 and Yb2.5, respectively. The Rp results (in μm) for alpha are among 0.0713 – 157, 0.0701 – 152, 0.0686 – 148, 0.0673 – 144 and 0.0655 – 125 for Yb0.5, Yb1.0, Yb1.5, Yb2.0 and Yb2.5, respectively. The order of Rp values for the glasses is as follows: Rpalpha<Rpproton<Rpelectron. Additionally, the largest Rp values of CPs follow the following order: Yb0.5 > Yb1.0 > Yb1.5 > Yb2.0 > Yb2.5. It is of significant importance to note that the glass with the highest density exhibits a lower Rp value, while the glass with the lowest density exhibits the greatest Rp value.

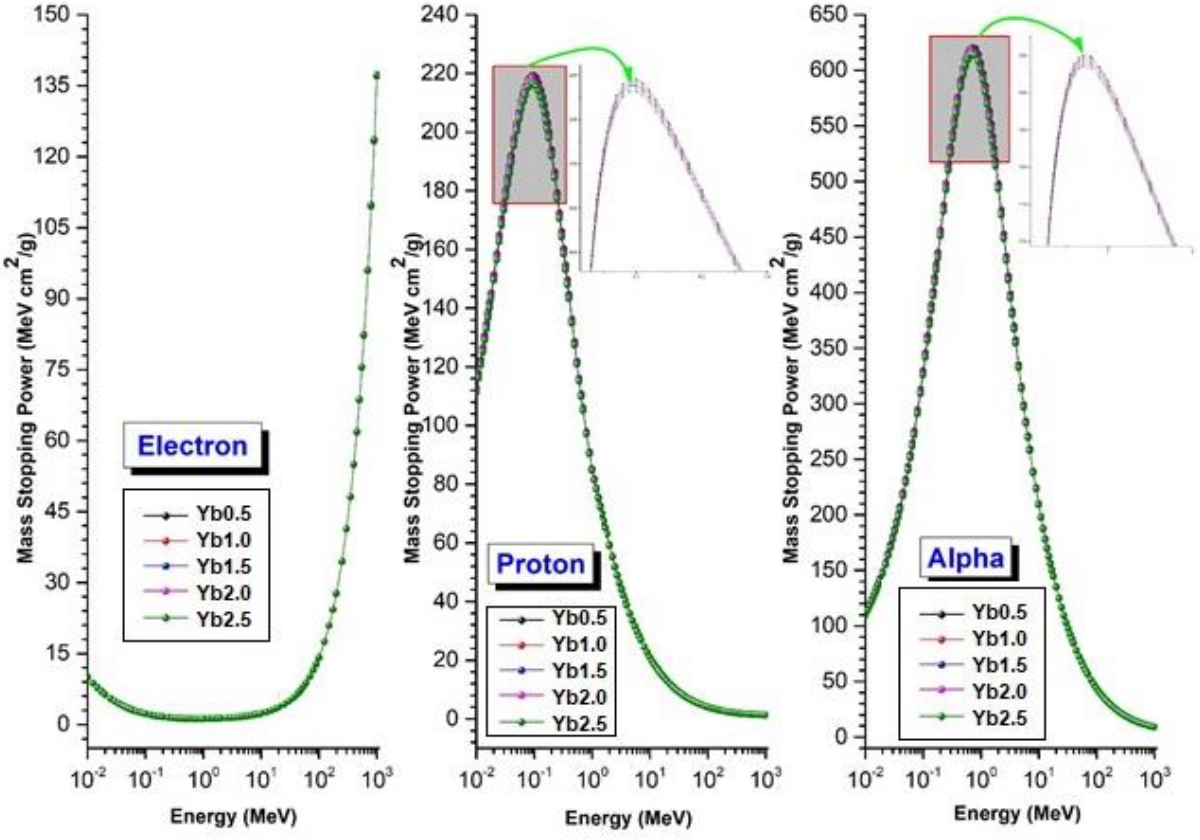

Figure 13. Dependence of MSP values of alpha, proton and electron particles versus the energy.

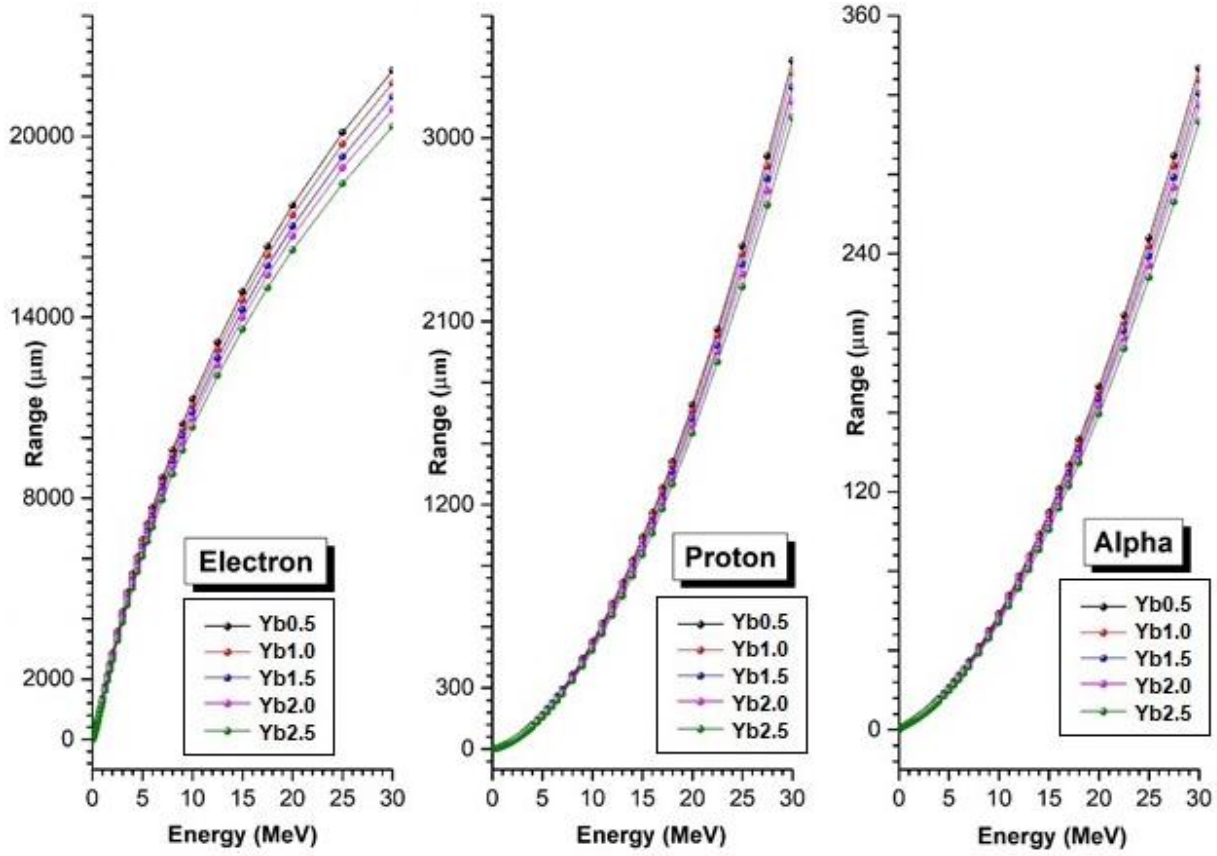

Figure 14. Changes of Rp values of alpha, proton and electron particles versus energy.

The Zeff results of the glasses are illustrated in Fig. 15. The Zeff values for electron are among 21.422 - 40.659, 21.623 - 40.804, 21.778 - 40.948, 21.925 - 41.091, 22.069 - 41.217 for Yb0.5, Yb1.0, Yb1.5, Yb2.0 and Yb2.5, respectively. The Zeff values for proton are among 12.185 - 24.951, 12.191 - 25.814, 12.196 - 26.041, 12.202 - 26.164, 12.207 - 26.265 for Yb0.5, Yb1.0, Yb1.5, Yb2.0 and Yb2.5, respectively. The Zeff results for alpha are among 13.447 - 38.556, 13.469 - 38.566, 13.703 - 38.576, 13.726 - 38.586, and 13.749 - 38.596 for Yb0.5, Yb1.0, Yb1.5, Yb2.0 and Yb2.5, respectively. From the results, the largest Zeff values of the glasses for all the CPs give the following order: Yb0.5 < Yb1.0 < Yb1.5 < Yb2.0 < Yb2.5. The Zeff values for electrons increase gradually with the kinetic energy for each sample. It has been documented that there is a non-monotonic variation in the behavior of alpha particles and protons in both low-and high-energy contexts. Furthermore, Zeff values tend to increase with increasing glass density.

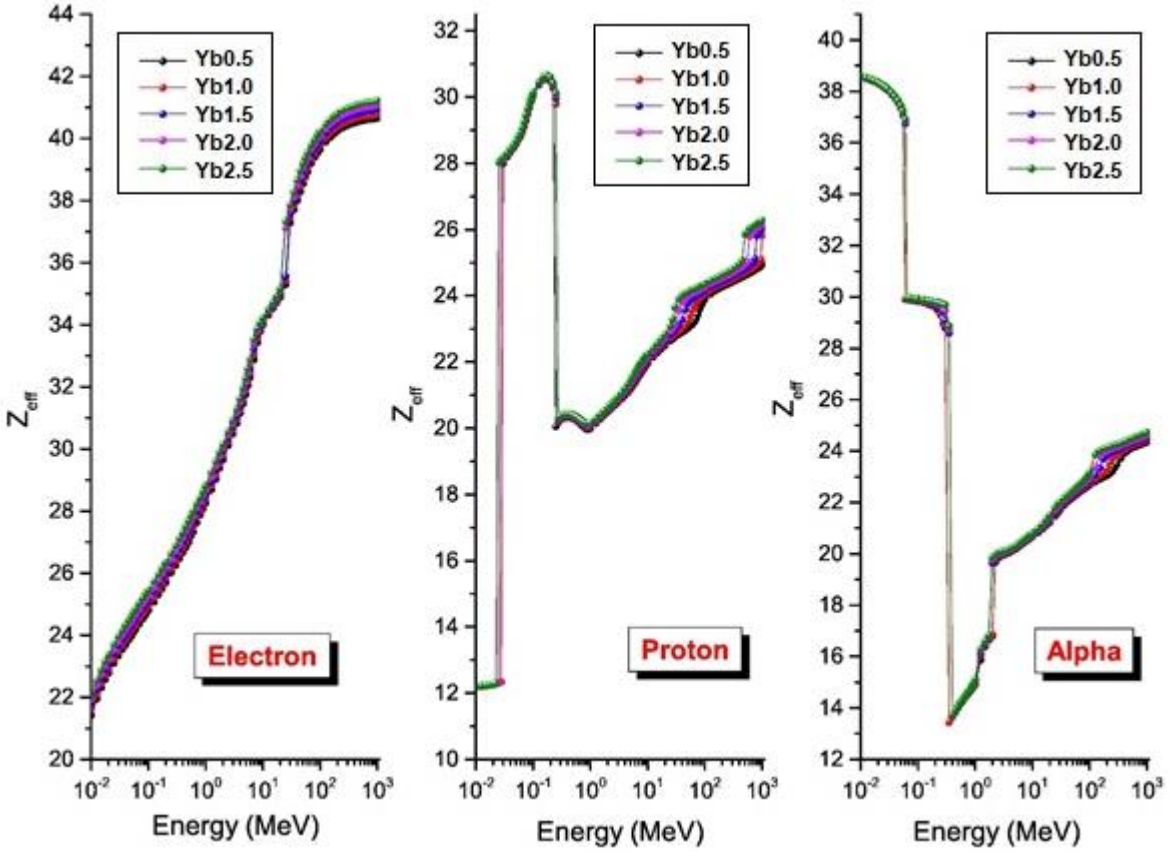

Figure 15. Variations of Z_{eff} values for alpha, proton and electron interactions with the studied glasses.

Also, the Neff results of the glasses for the CPs are calculated and demonstrated in Fig. 16. The Neff results (electrons/g) of electron are among 1.913 x 1023 – 3.632 x 1023, 1.921 x 1023 – 3.624 x 1023, 1.923 x 1023 – 3.617 x 1023, 1.926 x 1023 – 3.609 x 1023, 1.927 x 1023 – 3.600 x 1023 for Yb0.5, Yb1.0, Yb1.5, Yb2.0 and Yb2.5, respectively. The Neff values (electrons/g) of proton are among 1.088 x 1023 – 2.729 x 1023, 1.083 x 1023 – 2.716 x 1023, 1.077 x 1023 – 2.703 x 1023, 1.071 x 1023 – 2.691 x 1023, 1.066 x 1023 – 2.678 x 1023 for Yb0.5, Yb1.0, Yb1.5, Yb2.0 and Yb2.5, respectively. The Neff values (electrons/g) of alpha are among 1.201 x 1023 – 3.444 x 1023, 1.196 x 1023 - 3.426 x 1023, 1.210 x 1023 – 3.407 x 1023, 1.205 x 1023 – 3.389 x 1023, 1.201 x 1023 – 3.371 x 1023 for Yb0.5, Yb1.0, Yb1.5, Yb2.0 and Yb2.5, respectively. A similar pattern is observed in the Neff values as Zeff for electrons, which increase gradually with increasing kinetic energy for each glass sample. It is observed that non-monotonic variations in Neff values for alpha and proton are present in both low and high-energy regions.

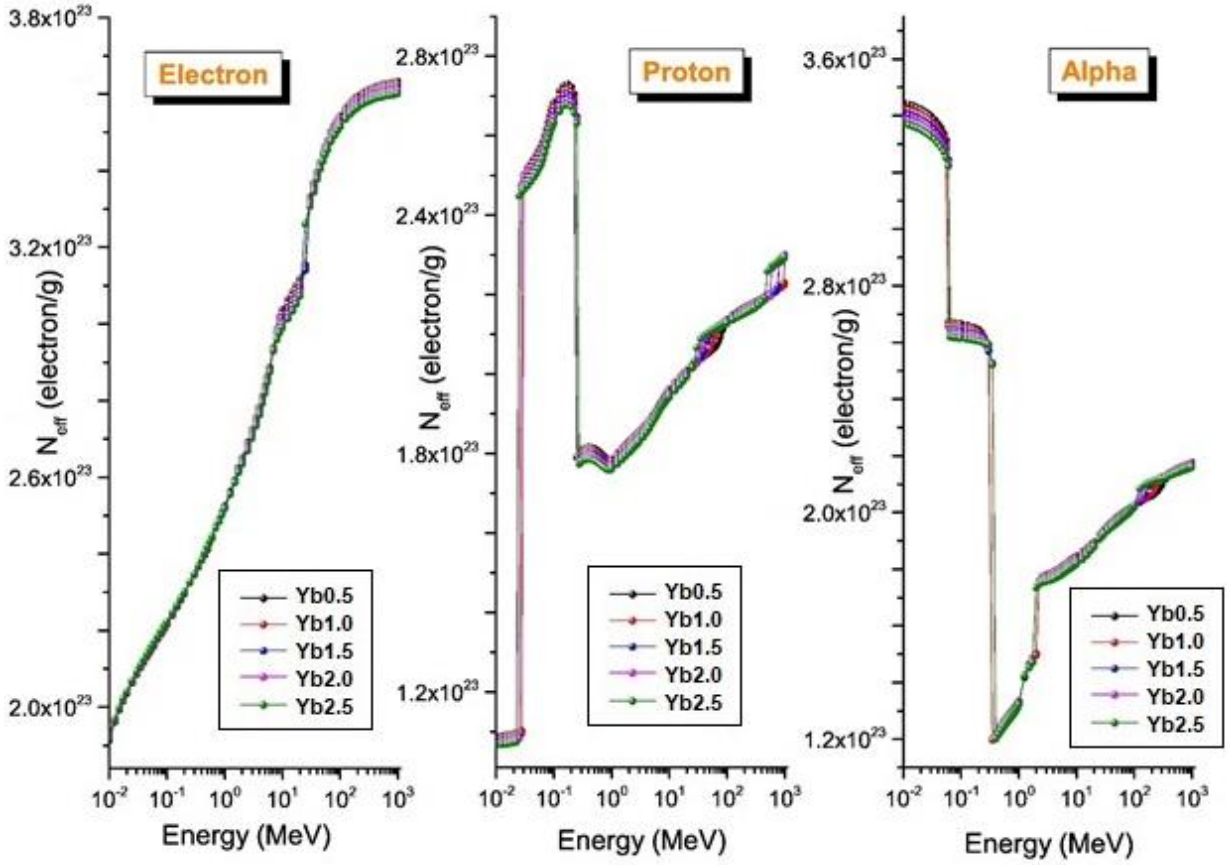

Figure 16. Variations of N_{eff} values for alpha, proton and electron interactions with the studied glasses.

4. CONCLUSIONS

In the paper, the radiation protection properties of Yb3+ doped glasses with contents of 50Bi2O3-15Li2O-15PbO-(20-x)B2O3-Yb2O3 (x = 0.5, 1.0, 1.5, 2.0 and 2.5 mol%) were examined for fast neutron, CPs and gamma-ray by Phy-X/PSD, PAGEX, ESTAR and SRIM codes. The MACVs, LACVs, MFP, HVL, ACS, ECS and Zeff values were evaluated and it was observed that these parameters exhibited energy-dependent behavior due to the photon interaction processes occurring across a broad spectrum of energies. In addition, the highest and lowest MACVs, LACVs, ACS, ECS, Zeff and μen values were found for Yb2.5 and Yb0.5 while those of MFPVs and HVLVs were determined for Yb0.5 and Yb2.5 glasses, respectively. Since the best neutron shielding value was obtained for Yb2.5 that has the highest FNRCS value among the glass samples, it can be explained that it is the glass with the best neutron shielding feature. The CPs' MSP results for the glasses are obtained in the order of alpha>proton>electron. The glass with the Yb0.5 composition recorded the longest Rp values for CPs, while the glass with Yb2.5 gave the shortest values. This difference can be assigned to the necessity of minimum thickness. The glasses subjected to investigation displayed an enhanced capability to shield against a range of CPs when Yb3+ was introduced. The study revealed that Yb2.5 offers the highest level of protection against gamma rays, neutrons and CPs, while Yb0.5 demonstrated the least effective performance among the glasses. It can be concluded that glasses with a higher proportion of Yb3+ provide a superior level of protection, while those with a lower proportion of Yb3+ offer a lesser degree of protection. As a result of this, it can be said that Yb3+ activated glasses with a composition of 50Bi2O3-15Li2O-15PbO-(20-x)B2O3-Yb2O3 can be applied as good shields for use in a wide range of applications. The results suggest that the investigated glasses with high Bi (Bi50) content and Yb+3 addition may have excellent radiation attenuation properties making them a promising option for radiation shielding applications. The attenuation of the RE-doped glasses is

a notable factor in achieving enhanced shielding, which in turn makes them appropriate for use in lighting technologies. It can thus be posited that Yb+3-doped glasses will prove instrumental in the advancement of material designs.

Declaration of Ethical Standards

Not applicable

Credit Authorship Contribution Statement

M. AYGUN: Conceptualization, Methodology, Writing original draft, Visualization, Investigation.
Z. AYGUN: Methodology, Writing original draft, Visualization, Investigation.
I. HAN: Writing original draft, Visualization, Investigation.
E. NARMANLI HAN: Writing- review, Visualization and editing.

Declaration of Competing Interest

The authors declare that they have no known competing financial interests or personal relationships that could have appeared to influence the work reported in this paper.

Funding

Not applicable

Data Availability

Data of this study are available from the corresponding author on responsible request.

5. REFERENCES

[1] M. Ahmadi, Z. Vahid, N. Darush, "Investigated mechanical, physical parameters and Gamma-Neutron radiation shielding of the rare earth (Er2O3/CeO2) doped barium borate glass: Role of the melting time and temperature," *Radiat. Phys. Chem., vol.* 217, p. 111450, 2024. https://doi.org/10.1016/j.radphyschem.2023.111450

[2] N. Almousa, S.A.M. Issa, A.S. Abouhaswa, H.M.H. Zakaly, "Improved radiation shielding efficiency and optical properties of borate glass by incorporating dysprosium(III) oxide," *Mater. Today Commun.*, vol. 39, p. 109198, 2024. https://doi.org/10.1016/j.mtcomm.2024.109198

[3] H.Al-Ghamdi, N.A.M. Alsaif, Z.Y. Khattari, A.A. El-Hamalawy,R. S. Diab, et al., "Development of Ce3+- and Yb3+-doped borate glasses for optical and radiation protection materials," *J. Mater. Sci.: Mater. Electron*, vol. 34, p. 1272, 2023. https://doi.org/10.1007/s10854-023-10687-1

[4] M. Aygun, "Gamma-ray, fast neutron and charged particle shielding performance of 15Li2O-25BaO-(40-x)B2O3-20P2O5-xDy2O3 glass system," *Radiat. Phys. Chem*., vol. 219, p. 111671, 2024. https://doi.org/10.1016/j.radphyschem.2024.111671

[5] P. Ramesh, Vinod Hegde, A.G. Pramod, B. Eraiah, D.A. Agarkov, G.M. Eliseeva, M.K. Pandey, K. Annapurna, G. Jagannath, M.K. Kokila, "Compositional dependence of red photoluminescence of Eu3+ ions in lead and bismuth containing borate glasses," *Solid State Sci.,* vol. 107, p. 106360, 2020. https://doi.org/10.1016/j.solidstatesciences.2020.106360.

[6] M. Pokhrel, G. A. Kumar, D. K. Sardar, " Highly efficient NIR to NIR and VIS upconversion in Er3+ and Yb3+ doped in M2O2S (M = Gd, La, Y)," *J. Mater. Chem. A*, vol. 38, pp. 11595-11606, 2013. https://doi.org/10.1039/C3TA12205K

[7] C. Wang, Xueqiang Liu, Kuan Peiwen, Peng Wang, Liyan Zhang, Danping Chen, "~1μm laser output based on heterogeneous fiber with Yb3+-doped fluorophosphate core and phosphate

cladding," *Mater. Letters*, vol. 179, pp. 9-11, 2016. https://doi.org/10.1016/j.matlet.2016.05.033.

[8] J. Bhemarajam, M. Varkolu, P. Syam Prasad, M. Prasad, "Effect of Yb3+ ions on spectroscopic and optical properties of Bi2O3–B2O3–Li2O–PbO glass system," *Results in Optics,* vol. 14, p. 100582, 2024, https://doi.org/10.1016/j.rio.2023.100582

[9] I.G. Geidam, K.A. Matori, M.K. Halimah, K.T. Chan, et al., "Thermo-physical and elastic properties of Bi2O3 doped silica borotellurite glasses," Optik, vol. 248, p. 168201, 2021. https://doi.org/10.1016/j.ijleo.2021.168201

[10] M. Kurudirek, N. Chutithanapanon, R. Laopaiboon, C. Yenchai, C. Bootjomchai, "Effect of Bi2O3 on gamma ray shielding and structural properties of borosilicate glasses recycled from high pressure sodium lamp glass," *J. Alloys Compd*., vol. 745, pp. 355-364, 2018. https://doi.org/10.1016/j.jallcom.2018.02.158

[11] K.A. Naseer, K. Marimuthu,, M.S. Al-Buriahib, A. Alalawic, H.O. Tekin, "Influence of Bi2O3 concentration on barium-telluro-borate glasses: Physical, structural and radiation-shielding properties," Ceramics Inter., vol. 47, pp. 329-340, 2021. https://doi.org/10.1016/j.ceramint.2020.08.138

[12] E.V. Malchukova, A.I. Nepomnyashchikh, B. Boizot, and E.I. Terukov, "Radiation Effects and Optical Properties of Aluminoborosilicate Glass Doped with RE Ions," *Glass Phys. Chem*., vol. 44, no. 4, pp. 356–363, 2018. https://doi.org/10.1134/S1087659618040090

[13] E.V. Malchukova, and B. Boizot, "Reduction of Eu3+ to Eu2+ in aluminoborosilicate glasses under ionizing radiation", *Mater. Res. Bull*., vol. 45, pp. 1299–1303, 2010. https://doi.org/10.1016/J.MATERRESBULL.2010.04.027

[14] G. Lakshminarayana, Ashok Kumar, H.O. Tekin, Shams A.M. Issa, M.S. Al-Buriahi, Dong-Eun Lee, Jonghun Yoon, Taejoon Park, "Binary B2O3–Bi2O3 glasses: scrutinization of directly and indirectly ionizing radiations shielding abilities," *J. Mater. Res. Technol*., vol. 9, no. 6, pp. 14549-14567, 2020. https://doi.org/10.1016/j.jmrt.2020.10.019.

[15] P. Vani, G. Vinitha, M.I. Sayyed, Maha M. AlShammari, N. Manikandan, "Effect of rare earth dopants on the radiation shielding properties of barium tellurite glasses," *Nucl. Engineer. Technol*., vol. 53, no. 12, pp. 4106-4113, 2021. https://doi.org/10.1016/j.net.2021.06.009.

[16] E.M. Abou Hussein, A. Sobhy, "Experimental investigation of new rare earth borosilicate glasses from municipal waste ash as high-dose radiation dosimeters," *Ceramics Inter*., vol. 50, no. 13, pp. 23012-23024, 2024. https://doi.org/10.1016/j.ceramint.2024.04.023.

[17] K.G. Mahmoud, M.I. Sayyed, A.S. Abouhaswa, "Optical and γ-ray absorption characteristics of Yb2O3-doped borate based glasses: a step towards understanding the substitution of B2O3/Yb2O3 in the lead borate glass system," *Physica Scripta*, vol. 98(11), 2023. http://dx.doi.org/10.1088/1402-4896/ad00e7

[18] H.H. Negm, A.A. Sdeek, A.A. Ebrahim, "The Role of Ytterbium (Yb2O3) in the Radiation Shielding Properties of Barium Titanium Borate Glasses (B2O3-TiO2-BaO) in Terms of γ and β Radiations," *J. Electronic Mater*., vol. 53, pp. 3965–3979, 2024. https://doi.org/10.1007/s11664-024-11073-1

[19] N. Tamam, Z.A. Alrowaili, I.O. Olarinoye, A. Hammoud et al., "Fabrication and characterisation of TeO2-based composite doped with Yb3+ and Bi3+ for enhanced radiation shielding safety," *Radiat. Phys. Chem*., vol. 215, p. 111315, 2024. https://doi.org/10.1016/j.radphyschem.2023.111315

[20] E. Şakar, Ö.F. Özpolat, B. Alım, M.I. Sayyed, M. Kurudirek, "Phy-X / PSD: Development of a user friendly online software for calculation of parameters relevant to radiation shielding and dosimetry," *Radiat. Phys. Chem.,* vol. 166, p. 108496, 2020. https://doi.org/10.1016/j.radphyschem.2019.108496

[21] J.F. Ziegler, "SRIM-The Stopping and Range of Ions in Matter,". http://www.srim.org.

[22] S. Prabhu, S. Jayaram, S.G. Bubbly, S.B. Gudennavar, "A simple software for swift computation of photon and charged particle interaction parameters: PAGEX," *Appl. Radiat. Isotopes,* vol. 176, p. 109903, 2021. https://doi.org/10.1016/j.apradiso.2021.109903

[23] I. Han, L. Demir, "Studies on effective atomic numbers, electron densities from mass attenuation coefficients in TixCo1−x and CoxCu1−x alloys," *Nucl. Instr. Methods in Phys. Res. Section B*, vol. 267, pp. 3505–3510, 2009. https://doi.org/10.1016/j.nimb.2009.08.022

[24] H.C. Manjunatha, "A study of gamma attenuation parameters in poly methyl methacrylate and Kapton," *Radiat. Phys. Chem.,* vol. 137, pp. 254–259, 2017. https://doi.org/10.1016/j.radphyschem.2016.01.024

[25] Y. Harima, "An historical review and current status of buildup factor calculations and applications," *Radiat. Phys. Chem.,* vol. 41, pp. 631–672, 1993.

[26] Y. Harima, Y. Sakamoto, S. Tanaka, M. Kawai, "Validity of the Geometric-Progression Formula in Approximating Gamma-Ray Buildup Factors," *Nucl. Sci. Engineer.,* vol. 94, pp. 24–35, 1986.

[27] ANSI/ANS 6.4.3 Gamma-ray Attenuation Coefficients and Buildup Factors for Engineering Materials. American Nucl Soc, La Grange Park, Illinois, 1991.

[28] K.R.M. Abdelgawad, G.S.M. Ahmed, A.T.M. Farag, A.A. Bendary, B.A. Tartor, I.I. Bashter, S.M. Salem, "Eco-friendly transparent glass prepared from rice straw ash for neutron and charged particle radiation shielding," *Annl. Nucl. Energy*, vol. 191, p. 109939, 2023. https://doi.org/10.1016/j.anucene.2023.109939

[29] M.F. L'Annunziata, "Nuclear Radiation, Its Interaction With Matter And Radioisotope Decay," *Handbook of Radioactivity Analysis*, pp. 1-122, 2003.

[30] M. Aygun, Z. Aygun., "A comprehensive analysis on radiation shielding characteristicsof borogypsum (boron waste) by Phy-X/PSD code," *Revista Mexicana de Fısica,* vol. 69, pp. 1–7, 2023. https://doi.org/10.31349/RevMexFis.69.040401

[31] I.I. Bashter, "Calculation of radiation attenuation coefficients for shielding concretes," *Annl. Nucl. Energy*, vol. 24, pp. 1389-1401, 1997. https://doi.org/10.1016/S0306-4549(97)00003-0

[32] G. Lakshminarayana, Y. Elmahroug, A. Kumar, H.O. Tekin, et al., "Detailed Inspection of γ-Ray, Fast and Thermal Neutrons Shielding Competence of Calcium Oxide or Strontium Oxide Comprising Bismuth Borate Glasses," *Mater.* vol. 14, p. 2265, 2021. https://doi.org/10.3390/ma14092265

[33] K.M. Kaky, M.I. Sayyed, M.K. Hamad, S. Biradar, M.H.A. Mhareb, U. Altimari, M.M. Taki, "Bismuth Oxide Effects on Optical, Structural, Mechanical, and Radiation Shielding Features of Borosilicate glasses," *Optical Mater.* https://doi.org/10.1016/j.optmat.2024.115853.

[34] M. Al-Buriahi, A. Abouhaswa, H. Tekin, C. Sriwunkum, F. El-Agawany, T. Nutaro, et al., "Structure, optical, gamma-ray and neutron shielding properties of NiO doped B2O3–BaCO3–Li2CO3 glass systems," *Ceram. Int.,* vol. 46, pp. 1711–1721, 2020. https://doi.org/10.1016/j.ceramint.2019.09.144.

[35] Y.S. Rammah, F.I. El-Agawany, A. Gamal, I.O. Olarinoye, E.M. Ahmed, A.S. Abouhaswa, "Responsibility of Bi2O3 Content in Photon, Alpha, Proton, Fast and Thermal Neutron Shielding Capacity and Elastic Moduli of ZnO/B2O3/Bi2O3 Glasses," *J. Inorganic Organometallic Polymers Mater.*, vol. 31, pp. 3505–3524, 2021. https://doi.org/10.1007/s10904-021-01976-5

[36] B.K. Jang, J.C. Lee, J.H. Kim, C.W. Chung, "Enhancement of thermal neutron shielding of cement mortar by using borosilicate glass powder," *Appl. Radiat. Isot.*, vol. 123, pp. 1-5, 2017. https://doi.org/10.1016/j.apradiso.2017.01.047